DOI:10.1021/jf900756d

JOURNAL OF AGRICULTURAL AND FOOD CHEMISTRY
ARTICLE

Antioxidant Oligostilbenoids from the Stem Wood of *Hopea hainanensis*

Hui-Ming Ge,† Wen-Hao Yang,† Jie Zhang, and Ren-Xiang Tan*

Institute of Functional Biomolecules, State Key Laboratory of Pharmaceutical Biotechnology, Nanjing University, Nanjing 210093, People's Republic of China. † These authors contributed equally to this work and therefore share co-first authorship.

Phytochemical investigation of the stem wood of *Hopea hainanensis*, a Dipterocarpaceae tree endemic to Hainan Island of China, leads to four new oligostilbenoids, hopeahainols C−F (**1**−**4**), and eight known ones (**5**−**12**). All of the structures were elucidated by comprehensive analysis of spectroscopic data including UV, IR, MS, and NMR after purification of individual compounds through a combination of chromatographic methods. A resveratrol glucoside, eight resveratrol dimers, two trimers, and a tetramer were identified. All of the polyphenols were tested for their radical scavenging and total reducing capacities by measuring their capacity to scavenge the 2,2-diphenyl-1-picrylhydrazyl (DPPH) radical, anion superoxide radical, and also to induce the reduction of Mo (VI) to Mo (V). Most of the compounds exhibited potent antioxidant and radical scavenger capacity compared with the positive controls (resveratrol, ascorbic acid, and butylated hydroxyanisole (BHA)) at 0.4 mM concentration.

KEYWORDS: *Hopea hainanensis*; resveratrol oligomers; polyphenols; structure elucidation; antioxidant; radical scavenging capacity

INTRODUCTION

There is increasing evidence to suggest that many degenerative or pathological processes, such as aging, cancer, and coronary heart disease, are related to reactive oxygen species (ROS) and radical-mediated reactions (*1*, *2*). Antioxidants can reduce oxidative damage to cells and biomolecules, defend against cancer-causing agents, and help lower the risk of cardiovascular disease, diabetes, and dementia including Alzheimer's disease (*3*, *4*). Searching for plant constituents with antioxidant properties leads to the discovery of new phytochemicals useful for the manufacture of functional food or medicine.

Resveratrol, a stilbene-based polyphenol, widely present in medicinal plants, grape skin, peanuts, and red wine, has been found to be substantially helpful for human health owing to its significant antioxidative actions (*5*−*7*) and is now widely used as additives in foods, cosmetics, and the pharmaceutical industry. Its oligomers have also received considerable chemical and biological attention because of their structural complexity as well as their array of bioactivities exhibited such as anticancer (*8*), antioxidative (*9*), anti-HIV (*10*), and antimicrobial (*11*) effects.

Plants belonging to the Dipterocarpaceae family, most of which are distributed in Southeast Asia, have been revealed to be a rich source of resveratrol oligomers (*12*−*15*). Research on the metabolites from the *Hopea* genus of the Dipterocarpaceae family has been carried out in our group. Several structurally novel oligostilbenoids have been isolated from the bark, which exhibited significant cytotoxic activity or potent inhibitory activity against acetylcholinesterase (*11*, *15*−*17*). In our further effort to search for antioxidant metabolites from *Hopea hainanensis*, four new oligostilbenoids together with eight known ones have been isolated from the ethanol extract of the stem wood, and their antioxidant properties have been also evaluated.

*To whom correspondence should be addressed. Tel: +86-25-8359-2945. Fax: +86-25-8330-2728. E-mail: rxtan@nju.edu.cn.

MATERIALS AND METHODS

Plant Material. *Hopea hainanensis* Merr. et Chun was collected in July 21, 2003 from the Botanical Garden of South China University of Tropical Agriculture with the specimen identified by Professor X. Q. Zheng (South China University of Tropical Agriculture). A voucher specimen (no. IFB030721) was deposited at Institute of Functional Biomolecules, Nanjing University, Nanjing, China.

Reagents and Instrumentation. All of the solvents used in the study, such as methanol, acetone, ethyl acetate, chloroform, and *n*-butanol, were of analytical grade and were purchased from Nanjing Chemical Reagent Co., Ltd., Nanjing, People's Republic of China. All deuteriated solvents, acetone-d_6, and dimethyl-d_6 sulfoxide for NMR measurement were purchased from Merck, Inc. Fourier transform NMR spectra were recorded at 500 MHz for ^{1}H and at 125 MHz for ^{13}C on a Bruker DRX-500 NMR spectrometer with tetramethylsilane (TMS) or solvent signals as internal references, at 25 °C. UV spectra were recorded on a Hitachi U-3000 spectrophotometer in MeOH solutions. IR spectra were measured on a Nexus 870 FT-IR spectrometer. HRESIMS were recorded using an Agilent 6210 TOF LC/MS equipped with an electrospray ionization (ESI) probe operating in positive or negative ion mode with direct infusion. HREIMS were recorded on a Micromass GCT TOF mass spectrometer equipped with an electron impact ionization (EI) probe with direct infusion. The semipreparative HPLC was performed using a 250 × 10 mm, 5 μm, Hypersil ODS column (Thermo Fisher Scientific, USA) on a Hitachi HPLC system consisting of a L-7110 pump (Hitachi) with a L-7420 UV/Vis Detector (Hitachi). Analytical TLC was performed on GF254 (10−20 mm) plates with 0.2 mm layer thickness. Column chromatography (CC) was performed on silica gel (200−300 mesh) or

 Published on Web 06/04/2009

Table 1. NMR Data of Compounds **1**−**4**[a]

	1[b]		**2**[c]		**3**[c]		**4**[c]	
	δ_C	δ_H (*J* in Hz)	δ_C	δ_H (*J* in Hz)	δ_C	δ_H (*J* in Hz)	δ_C	δ_H (*J* in Hz)
1a	123.5		132.9		130.9		130.8	
2a/6a	129.8	7.81(d, 8.4)	128.7	7.14(d, 8.4)	130.8	7.44(d, 8.3)	130.7	7.12(d, 7.8)
3a/5a	116.5	7.08(d, 8.4)	115.4	6.61(d, 8.4)	116.7	6.89(d, 8.3)	116.6	6.79(d, 7.8)
4a	159.2	8.94(−OH)	157.0	9.21(−OH)	159.1	9.68(−OH)	159.0	9.63(−OH)
7a	150.1		81.4	4.73(br s)	94.0	5.32(d, 11.0)	93.2	5.10(d, 10.9)
8a	125.1		45.8	4.37(br s)	46.9	3.96(d, 11.0)	45.6	2.19(d, 10.9)
9a	112.4		140.4		142.6		142.5	
10a	105.8	7.36(br s)	109.8	5.96(br s)	104.4	5.85(br s)	104.0	5.55(br s)
11a	158.1	8.67(−OH)	156.8	8.88(−OH)	157.6	9.09(−OH)	157.5	9.04(−OH)
12a	97.5	6.84(br s)	102.4	5.94(br s)	102.1	6.20(br s)	101.7	6.24(br s)
13a	154.9		158.4	8.60(−OH)	156.9	9.22(−OH)	156.8	9.51(−OH)
14a	124.3		115.6		117.6		115.8	
1b	123.5		136.9		131.2		129.2	
2b/6b	129.8	7.81(d, 8.4)	130.7	6.85(d, 8.2)	129.2	6.81(d, 8.2)	130.0	6.26(d, 7.6)
3b/5b	116.5	7.08(d, 8.4)	115.0	6.58(d, 8.2)	115.7	6.67(d, 8.2)	114.9	6.43(d, 7.6)
4b	159.2	8.94(−OH)	156.1	9.00(−OH)	157.8	9.33(−OH)	158.4	9.33(−OH)
7b	150.1		53.3	3.97(d,1.4)	88.9	4.47(d, 2.9)	86.0	4.42(br s)
8b	125.1		82.5	4.96(d,1.4)	47.3	4.27(d, 2.9)	45.5	4.57(br s)
9b	112.4		142.8		135.7		134.8	
10b	105.8	7.36(br s)	104.8	6.33(d, 1.2)	108.1	5.70(br s)	108.8	6.37(br s)
11b	158.1	8.67(−OH)	157.8	9.16(−OH)	158.3	9.03(−OH)	158.6	9.10(−OH)
12b	97.5	6.84(br s)	102.7	6.21(d, 1.2)	96.3	6.02(br s)	96.2	5.98(br s)
13b	154.9		153.1	9.30(−OH)	158.0		157.6	
14b	124.3		121.0		122.7		123.1	
15b					58.3	3.02(s)	57.3	3.24(s)

[a] Measured at 500 MHz for ^{1}H NMR and at 125 MHz for ^{13}C NMR. [b] Measured in acetone-d_6. [c] Measured in DMSO-d_6.

Sephadex LH-20 (Pharmacia Biotech, Uppsala, Sweden). Silica gel (200−300 mesh) and GF254 (10−20 mm) were produced by Qingdao Marine Chemical Factory, Qingdao, People's Republic of China.

Extraction, Isolation, and Purification Procedures of Bioactive Compounds. The air-dried and powdered stem woods of *H. hainanensis* (13.6 kg) were extracted with EtOH (3×20 L) at room temperature and concentrated in vacuo to give a crude extract (246.9 g), which was subsequently diluted with H_2O (500 mL) to give an aqueous suspension. After defatting by partitioning with *n*-hexane (3×500 mL), the suspension was extracted with EtOAc (3×500 mL). The EtOAc extract (182 g) was chromatographed on a silica gel column eluted with mixtures of $CHCl_3$/MeOH (100:0, 100:5, 100:10, 100:15, 100:20, 100:30, 100:40, 100:60, and 0:100, each 3.5 L) to give a total of 76 fractions (1−76). Fractions of similar compositions, as determined by TLC, were pooled, resulting in eight fractions: A (1−3), B (4−7), C (8−20), D (21−34), E (35−45), F (46−54), G (55−64), and H (65−76). Fraction C was subjected to passage over a second silica gel column, eluting with $CHCl_3$−MeOH increasing in polarity (100:5−100:20), to get fractions C1−C6. Fraction C1 was purified using Sephadex LH-20 eluted with MeOH to afford compound **1** (82.0 mg, 0.0006%). Fraction C4 was chromatographed on a Sephadex LH-20 column by elution with $CHCl_3$/MeOH (1:1) to obtain compound **7** (230.8 mg, 0.002%) and a mixture, which was further purified by silica gel column eluting with $CHCl_3$/MeOH (100:15) to obtain compound **8** (25.0 mg, 0.0002%). Fraction D was subjected to passage over a silica gel column, eluting with $CHCl_3$−MeOH increasing in polarity (100:10−100:30), to get fractions D1−D11. Gel filtration of fraction D5 using Sephadex LH-20 by elution with MeOH afforded compound **6** (7.1 mg, 0.00005%). Fraction D10 was resolved by preparative TLC chromatography eluting with $CHCl_3$/MeOH (5:1) to obtain **3** (7.6 mg, 0.00006%) and **4** (5.5 mg, 0.00004%). Gel filtration of fraction F over a Sephadex LH-20 column using MeOH yielded compounds **5** (7.5 mg, 0.00006%), **10** (10.7 mg, 0.00008%), and **11** (10.2 mg, 0.00008%). Residue of fraction F was subjected to RP-18 HPLC-UV using a MeOH/H_2O solution (55:45) and led to compounds **9** (25.1 mg, 0.0002%) and **2** (5.2 mg, 0.00004%). Compound **12** (23.8 mg, 0.0002%) was purified from fraction G using Sephadex LH-20 by elution with MeOH.

Hopeahainol C (**1**): green amorphous powder. UV (MeOH): λ_{max} (log ε): 223 (5.2), 255 (5.1), 402 (5.0) nm. IR (KBr) ν_{max}: 3539.2, 3414.1, 2923.6, 2851.9, 1631.0, 1611.6, 1584.4, 1510.9, 1433.1, 1383.6, 1373.0, 1305.8, 1270.5, 1238.2, 1223.5, 1168.5, 1132.1, 1108.9, 1068.5, 1050.6 1009.5, 983.4, 863.6, 826.2, 633.0, 519.7 cm^{-1}. ^{1}H and ^{13}C NMR spectroscopic data, see **Table 1**; HMBC and NOESY correlations, see Figures **2** and **3**; HREIMS *m*/*z* 448.0934 $[M]^+$ (calcd. for $[C_{28}H_{16}O_6]^+$, 448.0947).

Hopeahainol D (**2**): brown amorphous powder. UV (MeOH): λ_{max} (log ε): 230 (4.0, sh), 282 (4.2) nm. IR (KBr) ν_{max}: 3266.6, 2948.2, 1722.5, 1613.1, 1512.5, 1452.0, 1344.6, 1293.5, 1228.8, 1171.9, 1139.7, 1108.6, 1063.2, 1014.7, 942.7, 930.1, 819.9, 794.8 cm^{-1}. ^{1}H and ^{13}C NMR spectroscopic data, see **Table 1**; HMBC and NOESY correlations, see **Figures 2** and **3**; HRESIMS *m*/*z* 493.1252 $[M+Na]^+$ (calcd. for $[C_{28}H_{22}O_7Na]^+$, 493.1258).

Hopeahainol E (**3**): brown amorphous powder. UV (MeOH): λ_{max} (log ε): 228 (4.7, sh), 279 (4.2) nm. IR (KBr) ν_{max}: 3377.4, 2928.9, 2854.8, 1791.1, 1614.6, 1597.5, 1490.0, 1453.9, 1367.0, 1341.1, 1235.6, 1169.9, 1126.9, 1109.8, 1080.0, 1037.5, 1004.1, 974.8, 902.7, 833.1, 578.6, 522.8 cm^{-1}. ^{1}H and ^{13}C NMR spectroscopic data, see **Table 1**; HMBC and NOESY correlations, see **Figures 2** and **3**; HRESIMS *m*/*z* 507.1418 $[M+Na]^+$ (calcd for $[C_{29}H_{24}O_7Na]^+$, 507.1414).

Hopeahainol F (**4**): yellow amorphous powder. UV (MeOH): λ_{max} (log ε): 225 (4.7, sh), 283 (4.1) nm. IR (KBr) ν_{max}: 3330.6, 2932.3, 1613.4, 1513.6, 1491.2, 1455.1, 1342.9, 1229.8, 1171.6, 1125.8, 1093.5, 1003.1, 987.3, 906.3, 832.4, 579.7, 532.8 cm^{-1}. ^{1}H and ^{13}C NMR spectroscopic data, see **Table 1**; HMBC and NOESY correlations, see **Figures 2** and **3**; HRESIMS *m*/*z* 507.1412 $[M+Na]^+$ (calcd. for $[C_{29}H_{24}O_7Na]^+$, 507.1414).

Measurement of DPPH Radical Scavenging Capacity. According to the method of Brand-Williams (*18*), the scavenging capacity of metabolites was based on the reduction of methanolic DPPH$^\bullet$ in the presence of a hydrogen-atom-donating antioxidant. DPPH$^\bullet$ (4 mg, Sigma) was dissolved in 108 mL of MeOH. The investigated metabolites were prepared by dissolving 0.4 μmol of each compound in 1 mL of MeOH. Then, 38 μL of each solution-containing compound was added to 1.462 mL of DPPH$^\bullet$ solution at room temperature (*19*, *20*). The absorbance at 517 nm was measured after 30 min versus the blank (38 μL of MeOH in 1.462 mL of DPPH$^\bullet$ solution). Positive controls (containing natural antioxidant resveratrol and ascorbic acid, and synthetic antioxidant BHA (Sigma)) were also subjected to the same procedure for comparison. The analysis was carried out in triplicate, and the DPPH

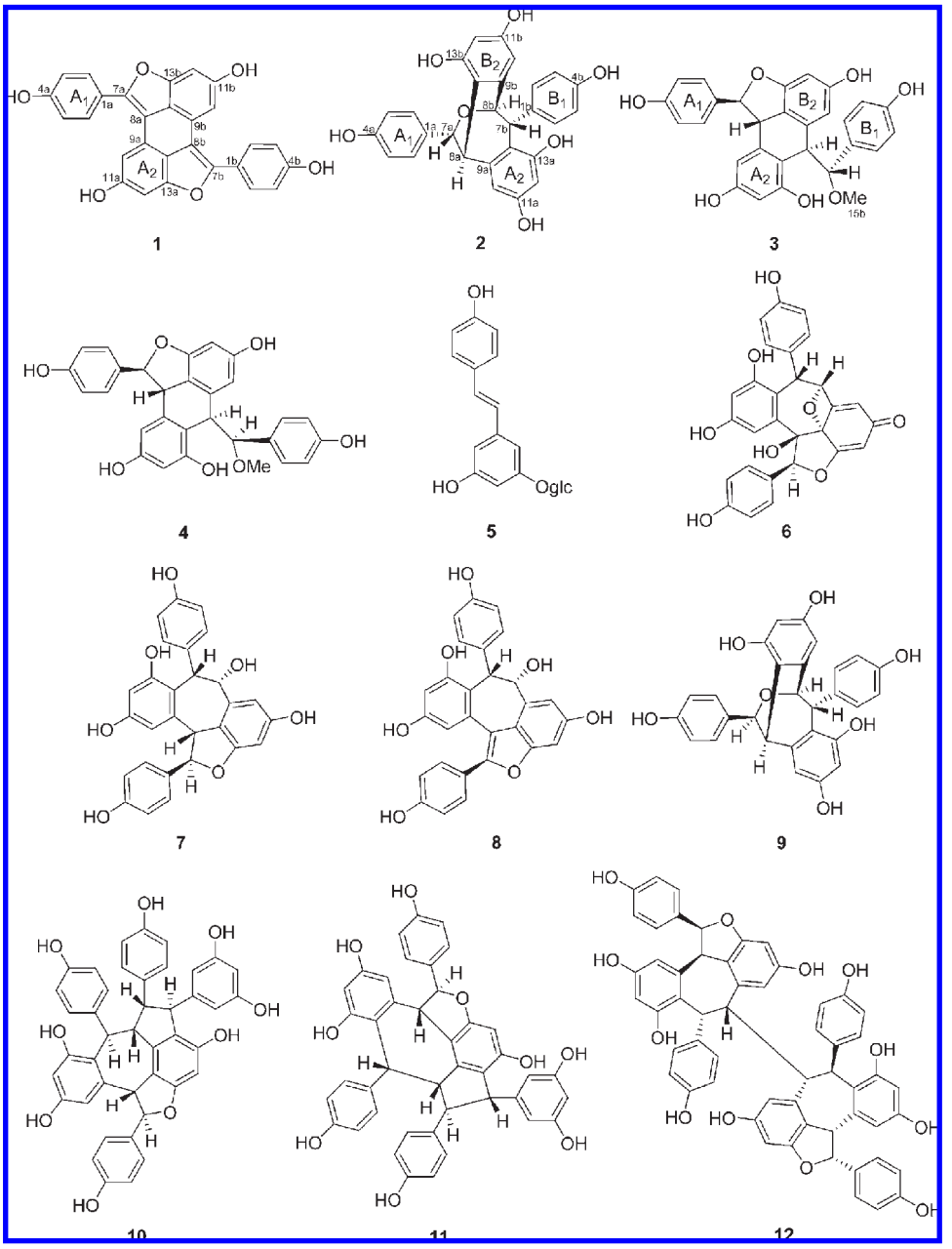

Figure 1. Sructures of oligostilbenoids isolated from *Hopea hainanensis*.

radical scavenging capacity (RSC, %) was calculated with the following equation: $(A517_{blank} - A517_{sample}) \div A517_{blank} \times 100\%$.

Measurement of Superoxide Radical Scavenging Capacity. The assay of superoxide radical scavenging capacity was based on the capacity of each isolated metabolite to inhibit the photochemical reduction of nitroblue tetrazolium (NBT) (BBI) in the riboflavin−light−NBT system (*21*). Each 3 mL reaction mixture contained 50 mM sodium phosphate buffer (pH 7.8), 13 mM methionine (BBI), 2 μM riboflavin (BBI), 100 μM EDTA, 75 μM NBT, and 100 μL of sample solution (0.4 mM in MeOH). The entire reactions were performed in an aluminum foil-lined box with two 20 W flurescent lamps. The distance between the reactant and the lamp was adjusted until the intensity of illumination reached about 4000lx. Identical tubes with reaction mixture were kept in the dark and serverd as blanks (*22*). The analysis was carried out in triplicate, and the results were expressed in terms of the percentage of RSC (%).

Evaluation of Total Reducing Capacity. Quantitative determination of antioxidant capacity was based on the reduction of Mo(VI) to Mo(V) by the sample analyte and the subsequent formation of a green phosphomolybdenum complex at acidic pH (*23*). Sample solutions (100 μL) containing reducing metabolites (0.4 mM in DMSO) were combined in an Eppendorf tube with 1 mL of reagent solution (0.6 M sulfuric acid, 28 mM sodium phosphate, and 4 mM ammonium molybdate, BBI). The tubes were capped and incubated in a thermal block at 95 °C for 90 min. After the samples had cooled to room temperature, the absorbance of an aqueous solution of each was measured at 695 nm against a blank (*19*). The analysis was carried out in triplicate, and increase of absorbance (△A695 nm) of the reaction mixture indicates the total antioxidant capacity.

RESULTS AND DISCUSSION

Structure Identification of the Isolated Compounds. The chemical structures of compounds **1**−**12** isolated from the organic extract of *Hopea hainanensis* are reported in **Figure 1**. All of the structures were elucidated on the comprehensive analysis of spectroscopic data including UV, IR, MS, and NMR.

Compound **1** was obtained as a green amorphous powder. Its IR absorption bands at 3414 (OH), 1584, and 1510 cm^{-1} (phenyl) indicated the present of phenolic hydroxyl groups. The $[M]^+$ ion peak at m/z 448.0934 in the HREIMS corresponded to a

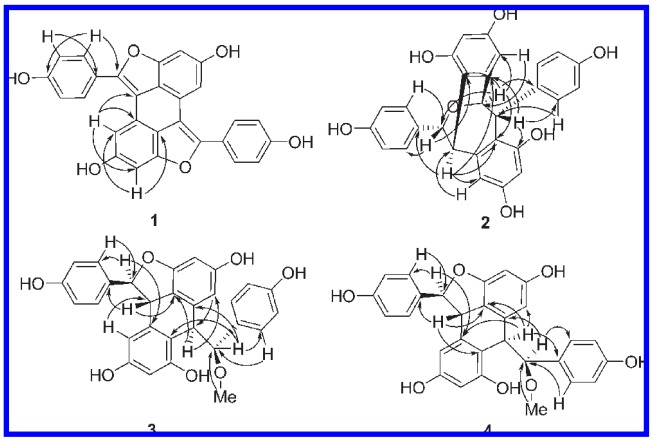

Figure 2. Selected HMBC correlations of compounds **1**−**4**.

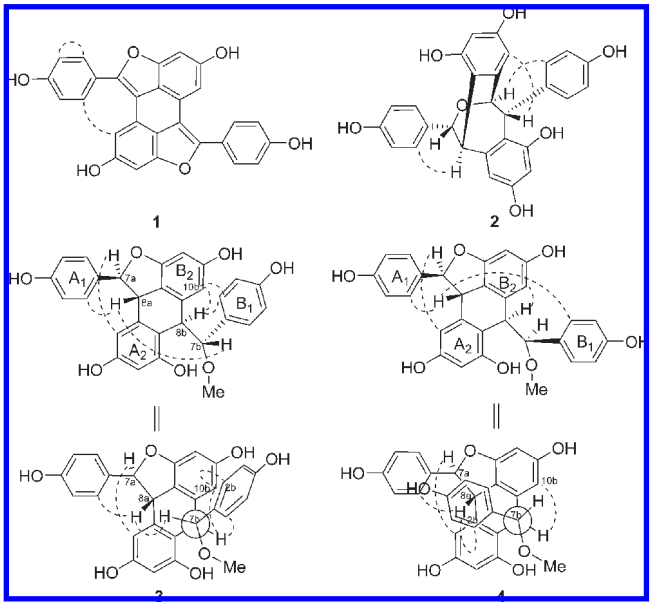

Figure 3. Selected NOE correlations of compounds **1**−**4**.

molecular formula of $C_{28}H_{16}O_6$ with 21 degrees of unsaturation. However, only 14 carbons and 8 protons were found in the ^{1}H NMR and ^{13}C NMR spectra, respectively, which suggested that compound **1** was a symmetrical dimer ($C_{14}H_8O_3 \times 2$). The ^{1}H and ^{13}C NMR spectrum showed the presence of a set of *ortho*-coupled protons assignable to a 4-hydroxyphenyl group [δ 7.81 (2H, d, J = 8.4 Hz, H-2a(6a)) and δ 7.08 (2H, d, J = 8.4 Hz, H-3a(5a))], a set of *meta*-coupled aromatic protons on a 1,2,3,5-tetrasubstituted benzene ring [δ 7.36 (1H, br s, H-10a) and δ 6.84 (1H, br s, H-12a)] and two hydroxyl groups (δ 8.94 and 8.67). HMBC correlations of H-2a(6a)/C-7a and H-8a/C-10a, together with the absence of sp^3 hybridized carbon signals in the ^{13}C NMR, suggested the presence of a stilbene skeleton (ring A_1-C-7a-C-8a-ring A_2). Subtracting 16 degrees of unsaturation (four phenyl rings) and 2 ones (two double bonds), compound **1** had three more rings. Except for two hydroxylated carbons [δ 159.2 (C-4a (4b)) and δ 158.1 (C-11a(11b))], two oxygenated carbons C-7a (7b) and C-13a(13b) resonating at δ 150.1 and 154.9 in ^{13}C NMR, respectively, revealed that C-7a(7b) and C-13b(13a) were linked through the last oxygen atom. Therefore, the remaining quaternary C-8a(8b) and C-14b(14a) were linked together to form the needed three rings. Thus, the planar structure of **1** was determined and illustrated as shown in **Figure 1**. It is noteworthy that hopeahainol C (**1**) is a highly unsaturated resveratrol dimer without chiral carbons.

Compound **2**, afforded as a brown amorphous powder, gave a $[M+Na]^+$ ion peak at m/z 493.1252 in the positive HRESIMS corresponding to the molecular formula $C_{28}H_{22}O_7$ ($[C_{28}H_{22}O_7Na]^+$, calcd. 493.1258). These data suggested that compound **2** could be a resveratrol dimer. The ^{1}H and ^{13}C NMR spectrum showed the presence of two sets of *ortho*-coupled protons assignable to two 4-hydroxyphenyl groups [δ 7.14 (2H, d, J = 8.4 Hz, H-2a(6a)) and δ 6.61 (2H, d, J = 8.4 Hz, H-3a(5a)); δ 6.85 (2H, d, J = 8.2 Hz, H-2a(6a)) and δ 6.58 (2H, d, J = 8.2 Hz, H-3a(5a))], two sets of *meta*-coupled aromatic protons on a 1,2,3,5-tetrasubstituted benzene ring [δ 5.96 (1H, br s, H-10a) and δ 5.94 (1H, br s, H-12a); δ 6.33 (1H, d, J = 1.2 Hz, H-10b) and δ 6.21 (1H, d, J = 1.2 Hz, H-12b)], and six phenolic hydroxyl groups [δ 9.03, 9.09, 9.22, 9.33, and 9.68]. Two sets of mutually coupled benzylic methine protons were also observed [δ 4.73 (1H, br s, H-7a) and δ 4.37 (1H, br s, H-8a); δ 3.97 (1H, d, J = 1.4 Hz, H-7b) and δ 4.96 (1H, d, J = 1.4 Hz, H-8b)]. Significant HMBC correlations of H-2a(6a) /C-7a, H-7a/C-2a(6a), H-8a/C-1a, H-8a/C-14a, H-8a/C-10a, H-10a/C-8a, H-10a/C-12a, H-10a/C-14a, H-12a/C-10a, and H-12a/C-14a revealed the presence of a stilbene skeleton (ring A_1-C7a-C8a-ring A_2), while another stilbene skeleton (ring B_1-C-7b-C-8b-ring B_2) was determined by HMBC correlations among H-2b(6b) /C-7b, H-7b/C-2b(6b), H-7b/C-9b, H-8b/C-1b, H-8b/C-10b, H-8b/C-14b, H-10b/C-8b, H-10b/C-12b, H-10b/C-14b, H-12b/C-10b, and H-12b/C-14b. The two stilbene skeletons could be connected by the linkages of C-8a/C-14b and C-14a/C-8b because of the HMBC correlations of H-8a/C-14b, H-7b/C-14a, and H-8b/C-14a. The one remaining oxygen atom was attributable to an ether bond between C-7a/C-8b according to a ^3J HMBC correlation between H-8b/C-7a. The planar structure of **2** shared the same skeleton with heimiol A (**9**) (*24*).

The relative configuration of compound **2** was unambiguously determined from its NOESY spectrum, as shown in **Figure 3**. The *trans* orientations of H-7a/H-8a and H-7b/H-8b were established by the distinctive NOEs among H-8a/H-2a(6a), H-8b/H-2b(6b), and H-7b/H-10b. H-7a and H-7b could be inferred as having a *cis* orientation to one another because of the geometrical requirement for the fusions of rings. Thus, compound **2** was determined as a 7a-stereoisomer of heimiol A and named hopeahainol D.

Hopeahainol E (**3**), afforded as a brown amorphous powder, had a molecular formula of $C_{29}H_{24}O_7$ established by the $[M+Na]^+$ ion peak at m/z 507.1418 in its HRESIMS. The polyphenolic nature of **3** was evidenced initially from its UV maxima centered at 235 and 283 nm. The ^{1}H and ^{13}C NMR data (**Table 1**) showed the presence of a methyl [δ 3.02 (3H, s, H-15b)], two sets of *ortho*-coupled protons assignable to two 4-hydroxyphenyl groups [δ 7.44 (2H, d, J = 8.3 Hz, H-2a(6a)) and δ 6.89 (2H, d, J = 8.3 Hz, H-3a(5a)); δ 6.81 (2H, d, J = 8.2 Hz, H-2a/H-6a) and δ 6.67 (2H, d, J = 8.2 Hz, H-3a/H-5a)], two sets of *meta*-coupled aromatic protons on a 1,2,3,5-tetrasubstituted benzene ring [δ 5.85 (1H, br s, H-10a) and δ 6.20 (1H, br s, H-12a); δ 5.70 (1H, br s, H-10b) and δ 6.02 (1H, br s, H-12b)], and five phenolic hydroxyl groups [δ 9.03, 9.09, 9.22, 9.33 and 9.68]. Two sets of mutually coupled benzylic methine protons were also observed [δ 5.32 (1H, d, J = 11.0 Hz, H-7a) and δ 3.96 (1H, d, J = 11.0 Hz, H-8a); δ 4.47 (1H, d, J = 2.9 Hz, H-7b) and δ 4.27 (1H, d, J = 2.9 Hz, H-8b)]. Significant HMBC correlations of H-2a(6a)/C-7a, H-7a/C-2a(6a), H-8a/C-1a, H-7a/C-9a, H-10a/C-8a, H-10a/C-12a, H-10a/C-14a, H-12a/C-10a, and H-12a/C-14a indicated the presence of a stilbene skeleton (ring A_1-C-7a-C-8a-ring A_2). Another stilbene skeleton (ring B_1-C-7b-C-8b-ring B_2) was revealed by HMBC correlations among H-2b(6b)/C-7b, H-7b/C-2b(6b), H-7b/C-9b, H-8b/C-10b, H-8b/C-14b, H-10b/C-8b, H-10b/

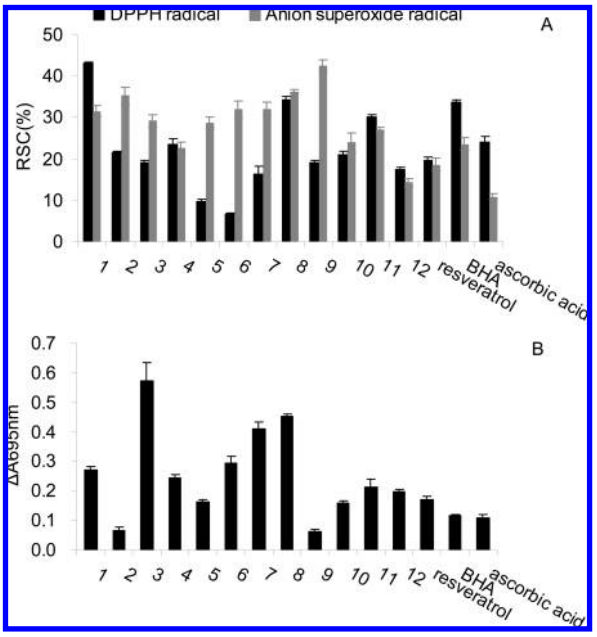

Figure 4. Antioxidant capacity of compounds **1**−**12**. (**A**) Radical scavenging capacity (RSC, %) on the DPPH radical and anion superoxide radical. (**B**) Total reducing capacity at ΔA695nm.

C-12b, H-10b/C-14b, H-12b/C-10b, and H-12b/C-14b. The two stilbene skeletons were connected by the linkages of C-8a/C-14b and C-14a/C-8b due to the HMBC correlations of H-8a/C-14b, H-7b/C-14a and H-8b/C-14a. Two remaining oxygen atoms were attributable to ether linkages between C-7a/C-13b and C-7b/C-15b(methyl) according to their characteristic chemical shift values and HMBC correlations of H-15b/C-7b. Thus, the planar structure of **3** was determined (**Figure 2**).

The relative configuration of compound **3** was determined from its NOESY data together with some upper field shift of protons. The *trans* orientation of H-7a/H-8a was unambiguously established by distinctive NOE between H-8a/H-2a(6a). The *trans* orientation of H-8b/H-8a could be determined by NOE correlation between H-8a and H-7b on the side chain. Although the chiral center of C-7b was located in a flexible side chain, the relative configuration of C-7b could be determined by NOE and its Newman projection. In the Newman projection of compound **3** (**Figure 3**), the bond between C-7b/C-8b is perpendicular to the plane formed by rings A_2 and B_2. NOE correlations were observed among H-2b(6b)/H-10b, H-2b(6b)/H-8b, and H-8a/H-7b, indicating the *trans* orientation of H-7b/H-8b (*25*). Furthermore, the proton signal of H-10b (δ 5.70) at relatively higher field caused by the anisotropy effect of ring B_1 also required this configuration of C-7b (*26*). Thus, the relative configuration of compound **3** was determined as shown in **Figure 3**.

Compound **4**, hopeahainol F, was afforded as a yellow amorphous powder. Its molecular formula was disclosed to be $C_{29}H_{24}O_7$ by HRESIMS with the ion detected at *m*/*z* 507.1412 $[M + Na]^+$ ($[C_{29}H_{24}O_7Na]^+$, calcd. 507.1414). As a reveratrol dimer, its ^{1}H- and ^{13}C NMR spectra (**Table 1**) were nearly identical with those of compound **3**, suggesting that compound **4** was one of the stereoisomers of **3**, which was unambiguously assigned by the interpretation of its ^{1}H-^{1}H COSY, HMQC, HMBC, and NOESY spectra (**Figure 2**).

The relative configuration of compound **4** was determined by a way similar that used for **3**. The *trans* orientations of H-7a/H-8a was established by a significant NOE correlation between H-8a/H-2a(6a). The *trans* orientation of H-8b/H-8a could be determined by the NOE correlation between H-8a and H-2b (6b) on the side chain. The NOE correlation between H-8a and H-2b(6b) and the absence of NOE between H-8b/H-2b(6b) indicated a *cis* orientation between H-7b/H-8b. In the Newman projection of compound **4**, H-8a is located below the benzene ring. Therefore, its chemical shift value (δ 2.19) was in an extraordinarily higher field because of the anisotropy effect of ring B_1. Thus, the relative stereochemistry of compound **4** was determined (**Figure 3**), which varied from that of **3** only by the configuration of C-7b.

In addition to four new compounds (**1**−**4**), eight known resveratrol oligomers were isolated, and their structures were identified as piceid (**5**), hopeahainanphenol (**6**) (*15*), balanocarpol (**7**) (*27*), malibatol A (**8**) (*10*), heimiol A (**9**) (*24*), vaticanol A (**10**) (*28*), vaticanol E (**11**) (*29*), and neoisohopeaphenol (**12**) (*15*), by spectral analyses and comparison with literature values.

Radical Scavenging and Total Reducing Capacities. The purity of the isolated compounds was determined of over 95% by using the HPLC-DAD method. All of the compounds were tested for their antioxidant properties by measuring their ability to scavenge radicals ($DPPH^•$ and $O_2^{•-}$) and by evaluating their total reducing capacity (to induce the formation of a phosphomolybdenum complex). The antioxidant capacity of compounds was compared with those shown by three known antioxidants: resveratrol, ascorbic acid, and BHA, treated in the same way. The antioxidant capacity of isolated compounds and positive controls was tested on the concentration of 0.4 mM in methanol or DMSO. The results are reported in **Figure 4**.

The DPPH radical is a stable radical with a maximum absorption at 517 nm that can easily undergo reduction by an antioxidant. Because of the ease and convenience of this reaction, it is now widely used in radical-scavening capacity assessment. The DPPH radical scavenging capacity of these resveratrol oligomers is shown in **Figure 4A**. Compounds **1** and **8** showed stronger capacities than BHA, while compounds **2**, **3**, **4**, **7**, **9**, and **11** showed capacities comparable to that of ascorbic acid. It is well accepted that the antioxidant ability of polyphenols is related to their hydroxyl group. The presence of a second hydroxyl group in the *ortho* or *para* position is known to increase the antioxidative ability due to additional resonance stability and *o*-quinone or *p*-quinone formation (*30*). It is also reported that the presence of the 4,4′-dihydroxy-*trans*-stilbene substructure can increase antioxidative ability (*31*). This may explain why compounds **1** and **8** are the most active radical scavenging agents.

The determination of superoxide radical scavenging capacity was based on the capacity of tested metabolites to inhibit the photochemical reduction of nitroblue tetrazolium (NBT) in the riboflavin−light−NBT system. As shown in **Figure 4A**, most of the resveratrol oligomers exhibited higher capacities than the positive controls on the concentration of 0.4 mM. The total reducing capacities of all isolated compounds are shown in **Figure 4B**. Most of the tested metabolites showed stronger reducing capacities than the three positive controls. Moreover, It is noteworthy that malibatol A (**8**) exhibited potent antioxidant property in all three models.

This study provides evidence that oligostilbenoids had interesting antioxidant properties expressed by their capacity to scavenge radicals and their total reducing capacity compared with that of resveratrol, ascorbic acid, and BHA, the widely used additives in the world. The present results suggest that these compounds, especially malibatol A (**8**), could be candidates for pharmaceutical use or food additives.

Supporting Information Available: ^{1}H NMR, ^{13}C NMR, HMQC, ^{1}H-^{1}H COSY, NOESY, HMBC, HRMS, and FT-IR

data. This material is available free of charge via the Internet at http://pubs.acs.org.

LITERATURE CITED

(1) Harman, D. Role of antioxidant nutrients in aging: overview. *Age* **1995**, *18*, 51–62.

(2) Gey, K. F. The antioxidant hypothesis of cardiovascular disease: epidemiology and mechanisms. *Biochem. Soc. Trans.* **1990**, *18*, 1041–1045.

(3) Tahirovic, I.; Sofic, E.; Sapcanin, A.; Gavrankapetanovic, I.; Bach-Rojecky, L.; Salkovic-Petrisic, M.; Lackovic, Z.; Hoyer, S.; Riederer, P. Brain antioxidant capacity in rat models of betacytotoxic-induced experimental sporadic Alzheimer's disease and diabetes mellitus. *J. Neural. Transm. Suppl.* **2007**, *72*, 235–240.

(4) Adhami, V. M.; Malik, A.; Zaman, N.; Sarfaraz, S.; Siddiqui, I. A.; Syed, D. N.; Afaq, F.; Pasha, F. S.; Saleem, M.; Mukhtar, H. Combined inhibitory effects of green tea polyphenols and selective cyclooxygenase−2 inhibitors on the growth of human prostate cancer cells both *in vitro* and *in vivo*. *Clin. Cancer Res.* **2007**, *13*, 1611–1619.

(5) Jang, M. S.; Cai, E. N.; Udeani, G. O.; Slowing, K. V.; Thomas, C. F.; Beecher, C. W. W.; Fong, H. H. S.; Farnsworth, N. R.; Kinghorn, A. D.; Mehta, R. G.; Moon, R. C.; Pezzuto, J. M. Cancer chemopreventive activity of resveratrol, a natural product derived from grapes. *Science* **1997**, *275*, 218–220.

(6) Olas, B.; Nowak, P.; Wachowicz, B. Resveratrol protects against peroxynitrite-induced thiol oxidation in blood platelets. *Cell. Mol. Biol. Lett.* **2004**, *9*, 577–587.

(7) Hung, L. M.; Chen, J. K.; Huang, S. S.; Lee, R. S.; Su, M. J. Cardioprotective effect of resveratrol, a natural antioxidant derived from grapes. *Cardiovasc. Res.* **2000**, *47*, 549–555.

(8) Ito, T.; Akao, Y.; Tanaka, T.; Iinuma, M.; Nozawa, Y. Vaticanol C, a novel resveratrol tetramer, inhibits cell growth through induction of apoptosis in colon cancer cell lines. *Biol. Pharm. Bull.* **2002**, *25*, 147–148.

(9) Kang, J. H.; Park, Y. H.; Choi, S. W.; Yang, E. K.; Lee, W. J. Resveratrol derivatives potently induce apoptosis in human promyelocytic leukemia cells. *Exp. Mol. Med.* **2003**, *35*, 467–474.

(10) Dai, J. R.; Hallock, Y. F.; Cardellina, J. H.; Boyd, M. R. HIV-inhibitory and cytotoxic oligostilbenes from the leaves of *Hopea malibato*. *J. Nat. Prod.* **1998**, *61*, 351–353.

(11) Ge, H. M.; Huang, B.; Tan, S. H.; Shi, D. H.; Song, Y. C.; Tan, R. X. Bioactive oligostilbenoids from the stem bark of *Hopea exalata*. *J. Nat. Prod.* **2006**, *69*, 1800–1802.

(12) Seo, E. K.; Chai, H.; Constant, H. L.; Santisuk, T.; Reutrakul, V.; Beecher, C. W. W.; Farnsworth, N. R.; Cordell, G. A.; Pezzuto, J. M.; Kinghorn, A. D. Resveratrol tetramers from *Vatica diospyroides*. *J. Org. Chem.* **1999**, *64*, 6976–6983.

(13) Ito, T.; Tanaka, T.; Iinuma, M.; Nakaya, K.; Takahashi, Y.; Sawa, R.; Murata, J.; Darnaedi, D. Three new resveratrol oligomers from the stem bark of *Vatica pauciflora*. *J. Nat. Prod.* **2004**, *67*, 932–937.

(14) Zgoda-Pols, J. R.; Freyer, A. J; Killmer, L. B.; Porter, J. R. Antimicrobial resveratrol tetramers from the stem bark of *Vatica oblongifolia* ssp. *oblongifolia*. *J. Nat. Prod.* **2002**, *65*, 1554–1559.

(15) Liu, J. Y.; Ye, Y. H.; Wang, L.; Shi, D. H.; Tan, R. X. New resveratrol oligomers from the stem bark of *Hopea hainanensis*. *Helv. Chim. Acta* **2005**, *88*, 2910–2917.

(16) Ge, H. M.; Xu, C.; Wang, X. T.; Huang, B.; Tan, R. X. Hopeanol: a potent cytotoxin with a novel skeleton *from Hopea exalata*. *Eur. J. Org. Chem.* **2006**, 5551–5554.

(17) Ge, H. M.; Zhu, C. H.; Shi, D. H.; Zhang, L. D.; Xie, D. Q.; Yang, J.; Ng, S. W.; Tan, R. X. Hopeahainol A: an acetylcholinesterase inhibitor from *Hopea hainanensis*. *Chem.—Eur. J.* **2008**, *14*, 376–381.

(18) Brand-Williams, W.; Cuvelier, M. E.; Berset, C. Use of a free radical method to evaluate antioxidant activity. *Lebensm.-Wiss. Technol.* **1995**, *28*, 25–30.

(19) Lu, Y. R.; Foo, L. Y. Antioxidant activities of polyphenols from sage (*Salvia officinalis*). *Food Chem.* **2001**, *75*, 197–202.

(20) Sroka, Z.; Cisowski, W. Hydrogen peroxide scavenging, antioxidant and anti-radical activity of some phenolic acids. *Food Chem. Toxicol.* **2003**, *41*, 753–758.

(21) Beauchamp, C.; Fridovich, I. Superoxide dismutase: improved assays and an assay applicable to acrylamide gels. *Anal. Biochem.* **1971**, *44*, 276–287.

(22) Dasgupta, N.; De, B. Antioxidant activity of *Piper betle* L. leaf extract *in vitro*. *Food Chem.* **2004**, *88*, 219–224.

(23) Prieto, P.; Pineda, M.; Aguilar, M. Spectrophotometric quantitation of antioxidant capacity through the formation of a phosphomolybdenum complex: specific application to the determination of vitamin E. *Anal. Biochem.* **1999**, *269*, 337–341.

(24) Weber, J. F.; Wahab, I. A.; Marzuki, A.; Thomas, N. F.; Kadir, A. A.; Hadi, A. H. A.; Awang, K.; Latiff, A. A.; Richommee, P.; Delaunaye, J. Heimiol A, a new dimeric stilbenoid from *Neobalanocarpus heimii*. *Tetrahedron Lett.* **2001**, *42*, 4895–4897.

(25) Adesanya, S. A.; Nia, R.; Martin, M. T.; Boukamcha, N.; Montagnac, A.; País, M. Stilbene derivatives from *Cissus quadrangularis*. *J. Nat. Prod.* **1999**, *62*, 1694–1695.

(26) Ohyama, M.; Tanaka, T.; Iinuma, M. Five resveratrol oligomers from roots of *Sophora leachiana*. *Phytochemistry* **1995**, *38*, 733–740.

(27) Tanaka, T.; Ito, T.; Idoa, Y.; Son, T. K.; Nakaya, K.; Iinuma, M.; Ohyama, M.; Chelladuraic, V. Stilbenoids in the stem bark of *Hopea parviflora*. *Phytochemistry* **2000**, *53*, 1015–1019.

(28) Tanaka, T.; Ito, T.; Nakayaa, K.; Iinumaa, M.; Riswan, S. Oligostilbenoids in stem bark of *Vatica rassak*. *Phytochemistry* **2000**, *54*, 63–69.

(29) Ito, T.; Tanaka, T.; Ido, Y.; Nakaya, K.; Iinuma, M.; Takahashi, Y.; Naganawa, H.; Riswan, S. Five new oligostilbenes with one or two dihydrofurans from the stem bark of *Vatica rassak*. *Heterocycles* **2001**, *55*, 557–567.

(30) Chen, J. H.; Ho, C.-T. Antioxidant activities of caffeic acid and its related hydroxycinnamic acid compounds. *J. Agric. Food Chem.* **1997**, *45*, 2374–2378.

(31) Cai, Y. J.; Fang, J. G.; Ma, L. P.; Yang, L.; Liu, Z. L. Inhibition of free radical-induced peroxidation of rat liver microsomes by resveratrol and its analogues. *Biochim. Biophys. Acta* **2003**, *1637*, 31–38.

Received March 5, 2009. Revised manuscript received May 10, 2009. Accepted May 15, 2009. This work was cosupported by grants for GHM from Natural Science Foundation of China (20802035), Natural Science Foundation of Jiangsu Province (BK2008270), and Ministry of Education (200802841022), and for TRX from Natural Science Foundation of China (30821006).